Robust kinase- and age-dependent dopaminergic and norepinephrine neurodegeneration in LRRK2 G2019S transgenic mice

Yulan Xiong[a,b,c,1], Stewart Neifert[a,b], Senthilkumar S. Karuppagounder[a,b,d], Qinfang Liu[c], Jeannette N. Stankowski[a,b,2], Byoung Dae Lee[a,b,3], Han Seok Ko[a,b,d,e], Yunjong Lee[a,b,4], Jonathan C. Grima[a,b,f], Xiaobo Mao[a,b], Haisong Jiang[a,b], Sung-Ung Kang[a,b], Deborah A. Swing[g], Lorraine Iacovitti[h,i], Lino Tessarollo[g], Ted M. Dawson[a,b,d,e,f,j,1], and Valina L. Dawson[a,b,d,e,f,k,1]

[a]Neuroregeneration and Stem Cell Programs, Institute for Cell Engineering, Johns Hopkins University School of Medicine, Baltimore, MD 21205; [b]Department of Neurology, Johns Hopkins University School of Medicine, Baltimore, MD 21205; [c]Department of Anatomy and Physiology, College of Veterinary Medicine, Kansas State University, Manhattan, KS 66506; [d]Adrienne Helis Malvin Medical Research Foundation, New Orleans, LA 70130-2685; [e]Diana Helis Henry Medical Research Foundation, New Orleans, LA 70130-2685; [f]Solomon H. Snyder Department of Neuroscience, Johns Hopkins University School of Medicine, Baltimore, MD 21205; [g]Neural Development Section, Mouse Cancer Genetics Program, Center for Cancer Research, National Cancer Institute, Frederick, MD 21702; [h]Department of Neuroscience, Thomas Jefferson University, Philadelphia, PA 19107; [i]Vickie and Jack Farber Institute for Neuroscience, Thomas Jefferson University, Philadelphia, PA 19107; [j]Department of Pharmacology and Molecular Sciences, Johns Hopkins University School of Medicine, Baltimore, MD 21205; and [k]Department of Physiology, Johns Hopkins University School of Medicine, Baltimore, MD 21205

Edited by Anders Björklund, Lund University, Lund, Sweden, and approved January 5, 2018 (received for review July 15, 2017)

Mutations in LRRK2 are known to be the most common genetic cause of sporadic and familial Parkinson's disease (PD). Multiple lines of LRRK2 transgenic or knockin mice have been developed, yet none exhibit substantial dopamine (DA)-neuron degeneration. Here we develop human tyrosine hydroxylase (TH) promoter-controlled tetracycline-sensitive LRRK2 G2019S (GS) and LRRK2 G2019S kinase-dead (GS/DA) transgenic mice and show that LRRK2 GS expression leads to an age- and kinase-dependent cell-autonomous neurodegeneration of DA and norepinephrine (NE) neurons. Accompanying the loss of DA neurons are DA-dependent behavioral deficits and α-synuclein pathology that are also LRRK2 GS kinase-dependent. Transmission EM reveals that that there is an LRRK2 GS kinase-dependent significant reduction in synaptic vesicle number and a greater abundance of clathrin-coated vesicles in DA neurons. These transgenic mice indicate that LRRK2-induced DA and NE neurodegeneration is kinase-dependent and can occur in a cell-autonomous manner. Moreover, these mice provide a substantial advance in animal model development for LRRK2-associated PD and an important platform to investigate molecular mechanisms for how DA neurons degenerate as a result of expression of mutant LRRK2.

LRRK2 | Parkinson's disease | neurodegeneration | α-synuclein

The G2019S (GS) mutation in leucine-rich repeat kinase 2 (LRRK2) is one of the most common genetic causes of Parkinson's disease (PD) (1–3). Multiple lines of transgenic or knockin mice expressing LRRK2 or disease-causing mutants have been generated. These animals have provided interesting biochemical and physiological insights, yet few have developed dopamine (DA)-neuron degeneration, a feature common to PD (4–21). LRRK2 is expressed at low levels in DA neurons in the substantia nigra pars compacta (SNpc), whereas it is expressed at higher levels in the caudate putamen (22–25). LRRK2 levels increase in activated microglia, where its activation may contribute to microglial-mediated degeneration of DA neurons (26–28). Thus, questions have been raised as to whether LRRK2 mediated DA neuron loss occurs in a cell-autonomous or non–cell-autonomous manner. Studies in culture model systems, viral transduction models, and *Drosophila* suggest that LRRK2 GS toxicity occurs in a kinase-dependent manner (19). To address the question of whether LRRK2 GS toxicity is cell-autonomous or non–cell-autonomous, as well as to address the role of kinase dependence, we generated tetracycline (Tet)-inducible conditional TetP-LRRK2 GS and TetP-LRRK2 GS kinase-dead (D1994A; TetP-LRRK2 GS/DA) mice under the control of a Tet-responsive regulator (20). To direct the expression of LRRK2 GS or LRRK2 GS/DA specifically in DA neurons, human tyrosine hydroxylase (TH) promoter-driven tTA (TH-tTA) mice were created. Cross-breeding TetP-LRRK2 GS or TetP-LRRK2 GS/DA mice with TH-tTA mice led to an age-dependent loss of DA neurons in the TH-tTA/LRRK2 GS mice but not in the TH-tTA/LRRK2 GS/DA mice, indicating that the LRRK2 GS kills DA neurons in a kinase-dependent manner and that loss of DA neurons occurs in a cell-autonomous manner.

Significance

The lack of a robust transgenic mouse model of loss of dopamine (DA) neurons has greatly hindered the study of Parkinson's disease caused by *LRRK2* mutations. In this manuscript, we report the development of catecholaminergic neuron-specific Tet-inducible conditional transgenic LRRK2 G2019S and LRRK2 G2019S kinase-dead transgenic mice, and show that LRRK2-induced DA and norepinephrine neurodegeneration is kinase-dependent and can occur in a cell-autonomous manner. Moreover, these models reveal that α-synuclein pathology is LRRK2 kinase-dependent and that there are LRRK2 kinase-dependent defects in clathrin-dependent endocytic trafficking that accompany mutant LRRK2-mediated neurodegeneration. These LRRK2 models have the potential to advance our understanding of mutant LRRK2-mediated degeneration of DA neurons.

Author contributions: Y.X., H.S.K., T.M.D., and V.L.D. designed research; Y.X., S.N., S.S.K., Q.L., J.N.S., B.D.L., Y.L., J.C.G., X.M., H.J., and S.-U.K. performed research; H.S.K., D.A.S., L.I., and L.T. contributed new reagents/analytic tools; Y.X., S.N., S.S.K., Q.L., J.N.S., B.D.L., Y.L., J.C.G., X.M., H.J., and S.-U.K. analyzed data; and Y.X., T.M.D., and V.L.D. wrote the paper.

The authors declare no conflict of interest.

This article is a PNAS Direct Submission.

[1]To whom correspondence may be addressed. Email: yulanxiong@ksu.edu, vdawson@jhmi.edu, or tdawson@jhmi.edu.

[2]Present address: Department of Neuroscience, Mayo Clinic, Jacksonville, FL 32224.

[3]Present address: Age-Related and Brain Disease Research Center, Department of Neuroscience, Kyung Hee University, Seoul 130-701, South Korea.

[4]Present address: Division of Pharmacology, Department of Molecular Cell Biology, Sungkyunkwan University School of Medicine, Samsung Biomedical Research Institute, Suwon 446-746, South Korea.

This article contains supporting information online at www.pnas.org/lookup/suppl/doi:10.1073/pnas.1712648115/-/DCSupplemental.

Results

Generation of TH-tTA Transgenic Mice. A tTA expression cassette was cloned downstream of the human TH promoter (29), and the integrity was verified by sequencing (Fig. 1*A*). TH-tTA transgenic mice were generated by pronuclear injections, and 23 positive founders were identified by PCR using tTA primers (Fig. S1 *A* and *B*). Three male mice (no. 99, no. 121, and no. 126) with the highest copy number were selected as founders and cross-bred to TetP-LRRK2 GS transgenic mice (Fig. S1 *C*–*E*) (20). Regional brain assessments of the overexpression of LRRK2 GS were monitored by Western blot analysis (Fig. S1 *C*–*E*). The TH-tTA line (no. 99) induced the highest LRRK2 expression levels in the striatum (STR) and ventral midbrain (VMB) and was therefore selected for subsequent studies. Founder mouse no. 99 was further cross-bred to histone 2Bj-GFP (TetP-H2Bj-GFP) reporter mice (30) and characterized (Fig. 1 *B*–*F*). Generation of double-transgenic mice was confirmed by PCR (Fig. 1*B*). Expression of nuclear-localized H2Bj-GFP is observed in TH-positive SNpc neurons (Fig. 1*C*). H2Bj-GFP is selectively expressed in DA neurons of the olfactory bulb (OB), VMB, and norepinephrine (NE) neurons of the locus coeruleus (LC), and no H2Bj-GFP is observed in the STR, cortex (CTX), hippocampus (HIP), or cerebellum (CER) (Fig. 1*D*). To confirm that the TH-tTA mice are doxycycline (DOX)-responsive, DOX was administered to the dams and maintained for 3 wk until weaning. A cohort of mice was maintained on DOX for 3 wk after weaning whereas DOX was withdrawn from a cohort of littermates. In mice maintained on DOX, there is no GFP expression, in contrast to mice in which DOX was withdrawn (Fig. 1 *E* and *F*).

Generation of Tet-Inducible Conditional LRRK2 Transgenic Mice with Expression Specifically in DA Neurons. We have generated Tet-responsive transgenic mice (TetP-LRRK2 GS or TetP-LRRK2 GS/DA) containing C-terminal tandem affinity purification-tagged human LRRK2 GS or LRRK2 GS/DA (20). Three of the highest copy-number male founder TetP-LRRK2 GS or TetP-LRRK2 GS/DA mice were cross-bred to the TH-tTA transgenic mice (Fig. 2*A*). Dams were maintained on DOX diet until pups were weaned to prevent expression of transgenes and the possibility of embryonic compensation during the development of DA neurons. Mice expressing both TH-tTA and TetP-LRRK2 GS or TetP-LRRK2 GS/DA were identified by PCR (Fig. 2*B*). At ∼2 mo of age, overexpression of LRRK2 GS or LRRK2 GS/DA was monitored by Western blot. LRRK2 GS is overexpressed 3.5-, 5.5-, and twofold in lines 648, 569, and 597, respectively, and LRRK2 GS/DA is overexpressed 5.3-, 5.3-, and 1.5-fold in lines 763, 767, and 768, respectively (Fig. 2 *C* and *D*). To screen for additional high expression of LRRK2 GS lines, we characterized an additional 38 TetP-LRRK2 GS founders under direction of the Tet promoter and selected two more high-expression lines, 674 and 492, at comparable levels as line 569 (Fig. S2). As lines 569 and 763 overexpress LRRK2 GS and LRRK2 GS/DA at similar levels, they were selected for further study. A regional assessment of the overexpression of LRRK2 GS or LRRK2 GS/DA was monitored by Western blot analysis (Fig. 2 *E* and *F*). LRRK2 GS and LRRK2 GS/DA are overexpressed 5- and 4.8-fold in the OB, 5- and 4.9-fold in the STR, as well as 6.3- and 6.5-fold in the VMB, whereas there is no significant change in LRRK2 expression in the CTX, HIP, CER, or BS (Fig. 2 *E* and *F*). LRRK2 GS and LRRK2 GS/DA are colocalized with TH-positive neurons in the SNpc, STR, and LC (Fig. 2*G* and Fig. S3). To confirm kinase activity in vivo, the phosphorylation status of LRRK2 was assessed in LRRK2 GS and LRRK2 GS/DA mice. Western blots of STR and VMB samples, respectively, from mouse brain reveal that LRRK2 GS has high phosphorylation levels as detected by antibodies to pS1292, but phosphorylation of LRRK2 in the LRRK2 GS/DA mice was undetectable (Fig. 2 *H* and *I*).

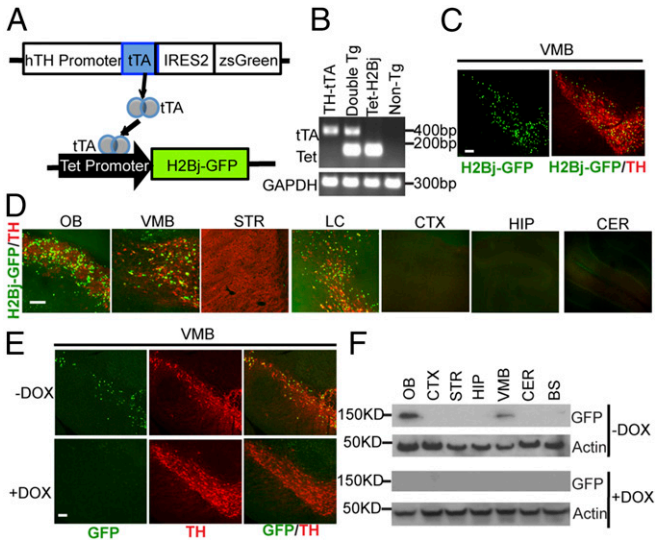

Fig. 1. Generation of TH-tTA transgenic mice. (*A*) Schematic diagram shows the generation of hTH-tTA/TetP-H2Bj-GFP double transgenic mice using the "Tet-off" system. (*B*) Representative genotyping PCR for TetP-H2Bj-GFP and hTH-tTA. GAPDH PCR was used as an internal control. (*C*) Representative images show the distribution of the nuclear-localized H2Bj-GFP fusion protein in midbrain coronal sections of hTH-tTA/TetP-H2Bj-GFP double-transgenic mice. (*D*) H2Bj-GFP (green) and TH (red) double staining in different mouse brain regions (sagittal sections; BS, brainstem). (*E*) Representative images of H2Bj-GFP expression in midbrain induced on DOX withdrawal for 3 wk (*Upper*) and suppressed by DOX administration (*Lower*). (*F*) Immunoblotting with GFP antibody for H2Bj-GFP expression in response to DOX. (Scale bar: 100 μm.)

Kinase-Dependent Loss of Catecholaminergic Neurons. DA neuronal number was assessed by unbiased stereological counting of TH- and Nissl-positive neurons at 10, 15, 20, and 24 mo of age. Significant DA neuronal loss in the SNpc of LRRK2 GS mice begins at 15 mo of age and progresses until 24 mo of age, when mice were euthanized (Fig. 3 *A*–*C*). Significant DA neuronal loss in the SNpc is also observed in the high-expressing LRRK2 GS line 674 (Fig. S4*A*). No significant DA neuronal loss is observed in LRRK2 GS/DA mice (Fig. 3 *A*–*C*) and line 648, which expresses lower levels of LRRK2 GS (Fig. S4*B*). Accompanying the loss of DA neurons in the LRRK2 GS mice is a reduction of DA and DA metabolites 3,4-dihydroxyphenylacetic acid (DOPAC) and homovanillic acid (HVA) in the STR as determined by HPLC (Fig. 3 *D* and *E*). No significant change in DA and DA metabolites DOPAC and HVA in the STR of LRRK2 GS/DA mice is observed (Fig. 3 *D* and *E*). No significant change in DA turnover or 5-hydroxytryptamine (5HT) and 5-hydroxyindoleacetic acid (5HIAA) in the STR of LRRK2 GS or GS/DA mice is observed (Fig. S5 *A* and *B*). NE neuronal loss is observed in the LC at 24 mo of age as assessed by unbiased stereological counting of TH- and Nissl-positive neurons in LRRK2 GS mice but not in LRRK2 GS/DA mice (Fig. 3 *F* and *G*). There was an insignificant loss of NE as determined by HPLC ($P = 0.0523$; Fig. S5*C*). Significant DA neuronal loss is also observed in the OB of LRRK2 GS mice compared with control mice, but an insignificant loss compared with LRRK2 GS/DA mice at 24 mo of age as assessed by unbiased stereological counting of TH neurons (Fig. S6). To evaluate whether there are other neuropathologic abnormalities, we examined the brains for astrocytosis. In 24-mo-old LRRK2 GS transgenic mice, there was a substantial increase in GFAP immunoreactivity in the SNpc and STR, consistent with the loss of DA neurons (Fig. 3*H*). There was no substantial difference in GFAP immunoreactivity in the LRRK2 GS/DA transgenic mice. Furthermore, there was no substantial

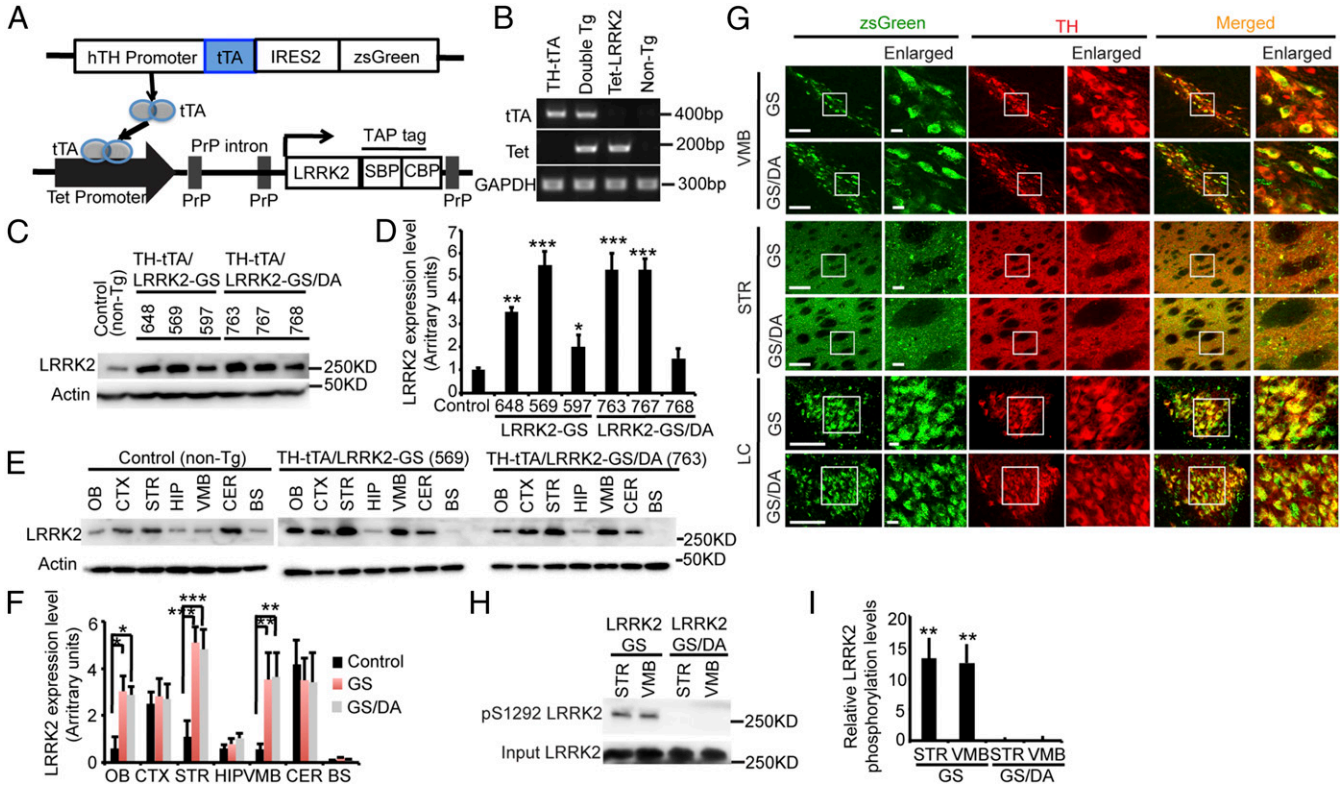

Fig. 2. Generation of Tet-inducible conditional LRRK2 transgenic mice with transgene expression specifically in catecholaminergic neurons. (*A*) Schematic diagram of the generation of LRRK2-inducible transgenic mice using the Tet-off system. (*B*) Representative genotyping PCR for TetP-LRRK2 and TH-tTA. GAPDH PCR was used as an internal control. (*C*) Western blot analysis of LRRK2 expression from hTH-tTA/TetP-LRRK2 transgenic mouse brains. Each number represents a single LRRK2 transgenic founder line. (*D*) Quantification of LRRK2 expression in mouse brains normalized to β-actin ($n = 3$). Significance was determined by one-way ANOVA [$F(6,14) = 17.6$; $P < 0.0001$] followed by Dunnett's post hoc test. (*E*) Representative Western blots of LRRK2 distribution in brain subregions from control, LRRK2-GS (line 569), and LRRK2-GS/DA (line 763) transgenic mice. (*F*) Quantification of LRRK2 distribution in mouse brains normalized to β-actin ($n = 3$). Significance was determined by two-way ANOVA [$F(6,42) = 12.41$; $P < 0.0001$] followed by Tukey's post hoc test. (*G*) Immunohistochemistry images of zsGreen (green) and TH (red) at VMB, STR, and LC subregions from coronal sections of LRRK2 GS and GS/DA transgenic mice. (Scale bars: low-magnification images, 100 μm; high-magnification images, 20 μm.) (*H*) Western blot analysis of total protein from pooled STR and VMB mouse tissue lysates of control, LRRK2 GS, and LRRK2 GS/DA probed with anti-LRRK2 and LRRK2 phospho-S1292 (pS1292) antibodies. (*I*) Quantification of pS1292 LRRK2 levels in mouse brains normalized to total LRRK2 protein level ($n = 3$). Significance was determined by was determined by one-way ANOVA [$F(3,8) = 13.12$; $P = 0.0019$] followed by Dunnett's post hoc test. Quantified data in *D*, *E*, and *I* are expressed as mean ± SEM (*$P < 0.05$, **$P < 0.01$, and ***$P < 0.001$).

difference in GFAP immunoreactivity in the CTX in the LRRK2 GS or LRRK2 GS/DA mice (Fig. 3*H*). Western blot analyses of GFAP levels confirmed a significant up-regulation of GFAP in the STR and VMB of 24-mo-old LRRK2 GS transgenic mice, but not in the LRRK2 GS/DA transgenic mice, and no change in the CTX of either genotype (Fig. 3 *I* and *J*). To evaluate whether there is microglia activation, we examined the levels of CD68 by immunostaining at 24 mo of age. No significant CD68 signals were observed in the STR, VMB, and CTX of LRRK2 GS, GSDA, and control mice (Fig. S7).

Reduced SVs and Accumulation of Clathrin-Coated Vesicles at DA Terminals. To determine whether there are changes at the DA nerve terminals in the STR, EM analysis was performed. At 24 mo of age, there is a significant reduction in synaptic vesicle (SV) number in the LRRK2 GS mice compared with nontransgenic and LRRK2 GS/DA mice (Fig. S8 *A* and *B*). The reduction in SV number is specific to DA neurons as determined by immunogold VMAT2 staining of DA nerve terminals (Fig. S8*D*). Interestingly, a much greater abundance of clathrin-coated vesicles (CCVs) is observed at synapses of LRRK2 GS mice relative to LRRK2 GS/DA mice (Fig. S8 *A* and *C*).

Behavioral Deficits. The motor function of transgenic mice by rotarod, open-field, pole test, and gait analysis was examined. The LRRK2 GS and LRRK2 GS/DA transgenic mice performed normally on the rotarod (Fig. S9*A*) and in the open-field test at 15 and 24 mo of age (Fig. 4*A*). Open-field testing at 24 mo was monitored after d-amphetamine administration (7 mg/kg s.c.). Nontransgenic and LRRK2 GS/DA mice exhibit increased activity, whereas the LRRK2 GS mice exhibit a blunted response (Fig. 4*A*). Stride length in the LRRK2 GS mice is reduced at 24 mo of age, but is unchanged in the LRRK2 GS/DA mice. All three strains of mice have normal stride length at 15 mo of age (Fig. 4*B*). In a DA-sensitive pole test assessed at 10, 15, and 24 mo of age, LRRK2 GS transgenic mice exhibited deficits in climbing down the pole at 24 mo of age. The LRRK2 GS/DA mice performed similarly to nontransgenic control mice (Fig. 4*C*). Transgenic mice were administered levodopa (L-Dopa), and the pole test deficits seen in 24-mo-old LRRK2 GS mice were ameliorated (Fig. 4*D*). Taken together, these results indicate that the LRRK2 GS mice have DA-sensitive behavioral deficits.

LRRK2 Kinase-Dependent α-Synuclein Pathology. As the majority of patients carrying the LRRK2 GS mutation have α-synuclein–positive Lewy bodies and increased phospho-serine 129 (pS129) α-synuclein, pS129 α-synuclein levels were assessed. Low levels of immunoreactivity for pS129 α-synuclein are observed in the LRRK2 GS mice at 15 mo of age and are further elevated at 24 mo of age, whereas no immunoreactivity is observed in the

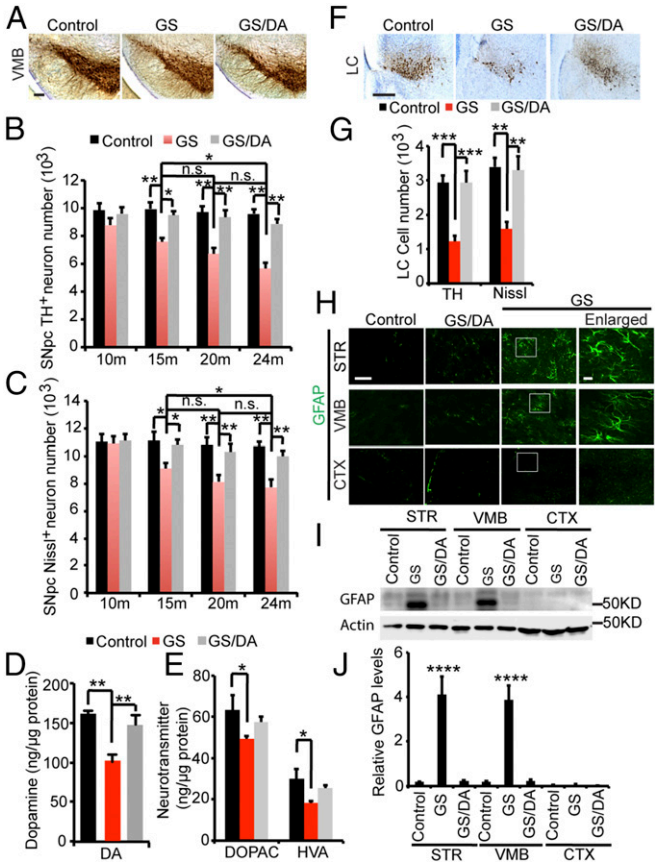

Fig. 3. Kinase-dependent loss of catecholaminergic neurons in conditional LRRK2-G2019S transgenic mice. (*A*) Representative TH immunohistochemistry of the midbrain coronal sections of 20-mo-old LRRK2 GS and GSDA transgenic and age-matched littermate controls. (Scale bar: 100 μm.) (*B*) Stereological assessment of TH-positive neurons in the SNpc (control, $n = 8$; GS, $n = 9$; GS/DA, $n = 8$). Significance was determined by two-way ANOVA [$F(3,92) = 5.762$; $P = 0.0012$] followed by Tukey's post hoc test. (*C*) Stereological assessment of Nissl-positive neurons in the SNpc (control, $n = 8$; GS, $n = 9$; GS/DA, $n = 8$). Significance was determined by two-way ANOVA [$F(3,88) = 5.254$; $P = 0.0022$] followed by a Tukey's post hoc test. (*D*) Striatal DA levels were analyzed by HPLC in controls and LRRK2 GS and GS/DA transgenic mice at 24 mo of age ($n = 5$). Significance was determined by one-way ANOVA [$F(2,12) = 9.055$; $P = 0.004$] followed by a Tukey's post hoc test. (*E*) DOPAC and HVA levels were analyzed by HPLC in controls and LRRK2 GS and GS/DA transgenic mice at 24 mo of age ($n = 5$). Significance was determined by one-way ANOVA [DOPAC, $F(2,6) = 4.854$, $P = 0.05$; HVA, $F(2,6) = 4.955$, $P = 0.4981$] followed by Tukey's post hoc test. (*F*) Representative TH immunohistochemistry of the LC coronal sections of 24-mo-old LRRK2 GS and GSDA transgenic and age-matched littermate controls. (Scale bar: 100 μm.) (*G*) Stereological assessment of TH- and Nissl-positive neurons in the LC ($n = 5$). Significance was determined by one-way ANOVA [TH, $F(2,12) = 15.87$, $P = 0.0004$; Nissl, $F(2,12) = 11.49$, $P = 0.0016$] followed by Tukey's post hoc test. (*H*) Representative GFAP immunohistochemistry of the STR, VMB, and CTX coronal sections of 24-mo-old LRRK2 GS and GSDA transgenic and age-matched littermate controls. (Scale bars: low-magnification images, 100 μm; high-magnification images, 20 μm.) (*I*) Representative GFAP immunoblotting of the STR, VMB, and CTX coronal sections of 24-mo-old LRRK2 GS and GSDA transgenic and age-matched littermate controls. (*J*) Quantification of GFAP levels in STR, VMB, and CTX mouse brain subregions normalized to actin levels. Significance was determined by two-way ANOVA [$F(2,18) = 17.7$; $P < 0.0001$] followed by Tukey's post hoc test. Quantified data in *B–E*, *G*, and *J* are expressed as mean ± SEM (*$P < 0.05$, **$P < 0.01$, and ***$P < 0.001$, ****$P < 0.0001$; n.s., not significant).

LRRK2 GS/DA mice (Fig. 5*A*). Immunoblot analysis for in the Triton-X100–soluble fraction reveals no substantial difference in the immunoreactivity for α-synuclein and pS129 α-synuclein at 15 and 24 mo of age between LRRK2 GS mice and LRRK2 GS/DA mice (Fig. 5*B*). However, in the Triton-X100–insoluble fraction, pS129 α-synuclein and high molecular weight species of α-synuclein are detected in the STR and VMB of LRRK2 GS mice at 15 and 24 mo of age, but not at 10 mo of age (Fig. 5 *C–E* and data not shown). No pS129 α-synuclein and high molecular weight species of α-synuclein are detected in the STR and VMB in the nontransgenic or the LRRK2 GS/DA mice at 15 and 24 mo of age (Fig. 5 *C–E*).

Discussion

We find that transgenic expression of LRRK2 GS in catecholaminergic neurons is sufficient to elicit age-dependent and kinase-dependent neurodegeneration, indicating that DA and NE neuronal loss as a result of LRRK2 GS can occur in a cell-autonomous manner. Accompanying the loss of DA neurons are deficits in DA and DA metabolites, reduced SVs and accumulation of CCV at DA terminals, deficits in DA-associated behaviors, and expression of pathologic phosphorylation and high molecular weight species of endogenous α-synuclein. Moreover, a powerful transgenic tool for Tet-sensitive expression for transgene expression in DA neurons was developed, the TH-tTA mice.

Numerous transgenic models for LRRK2 disease-causing mutations have been developed and described (4–21, 31). Most models exhibit biochemical, physiologic, and behavioral abnormalities without loss of DA neurons. The lack of DA neurodegeneration in these lines of mice might be a result of several factors, including the constitutive expression of the LRRK2 transgenes permitting compensation during the development of DA neurons, the modest

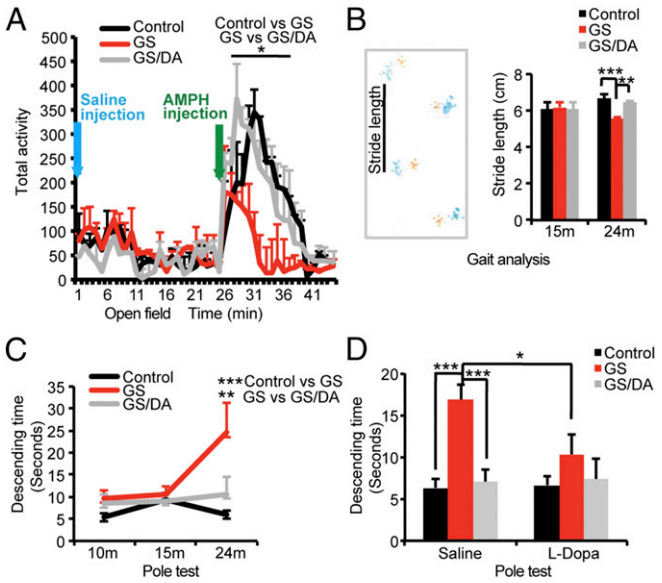

Fig. 4. Behavioral deficits of conditional LRRK2-G2019S transgenic mice. (*A*) Open-field analysis under normal conditions following saline solution injection and then following amphetamine challenge of 24-mo-old LRRK2 GS and GS/DA transgenic and age-matched littermate controls (control, $n = 9$; GS, $n = 9$; GS/DA, $n = 8$). Significance was determined by two-way ANOVA [$F(43,1012) = 8.473$; $P < 0.0001$] followed by Tukey's post hoc test. (*B*) Gait analysis by footprint analysis (control, $n = 9$; GS, $n = 9$; GS/DA, $n = 8$). Significance at 24 mo was determined by one-way ANOVA [$F(2,23) = 12.21$; $P = 0.0002$] followed by Tukey's post hoc test. (*C*) Pole test to monitor behavioral abnormalities (control, $n = 9$; GS, $n = 9$; GS/DA, $n = 8$). Significance was determined by one-way ANOVA [$F(2,23) = 4.429$; $P = 0.0236$] followed by Tukey's post hoc test. (*D*) Pole test with or without L-Dopa treatment of 24-mo-old LRRK2 transgenic mice and age-matched littermate controls (control, $n = 9$; GS, $n = 9$; GS/DA, $n = 8$). Significance was determined by two-way ANOVA [$F(2,23) = 16.83$; $P < 0.0001$] followed by Tukey's post hoc test. Data are the mean ± SEM (*$P < 0.05$, **$P < 0.01$, and ***$P < 0.001$).

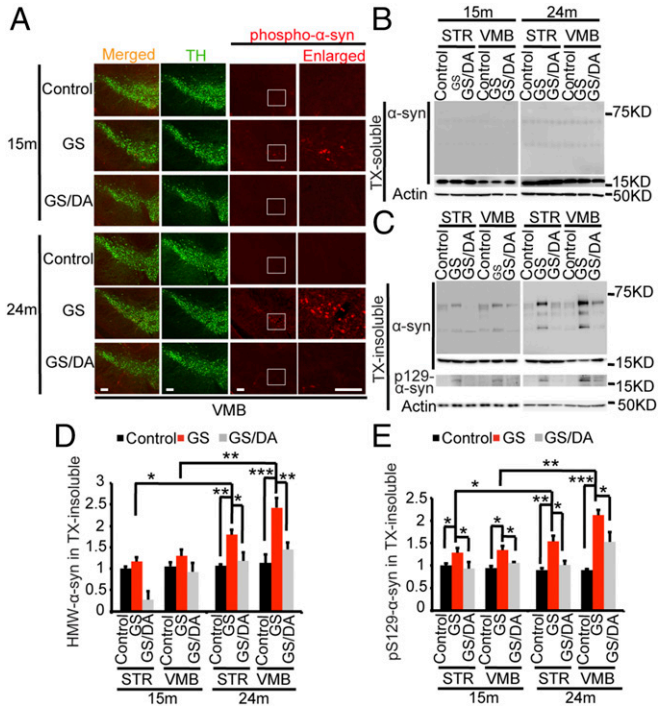

Fig. 5. α-Synuclein pathology of conditional LRRK2-G2019S transgenic mice. (*A*) Representative immunohistochemistry images of pS129 α-syn (red) and TH (green) at SNpc from LRRK2 GS and GS/DA transgenic mice and age-matched littermate non-Tg controls. (Scale bars: 100 μm.) (*B*) Representative immunoblots of α-syn and β-actin in the Triton-X100 (TX)-soluble fraction of the STR and VMB brain regions from 15- and 24-mo-old transgenic mice and age-matched littermate controls. (*C*) Representative immunoblots of α-synuclein and β-actin in the TX-insoluble fraction of the STR and VMB brain regions from 15- and 24-mo-old transgenic mice and age-matched littermate controls. In the insoluble fractions, high molecular weight (75 kDa) species of α-synuclein are detected in STR and VMB of LRRK2 GS mice. (*D*) Quantification of high molecular weight (HMW) α-synuclein protein levels in *C* normalized to β-actin ($n = 3$). Significance was determined by two-way ANOVA [STR-24m, $F(2,6) = 8.225$, $P = 0.0191$; VMB-24m, $F(2,6) = 11.6$, $P = 0.0087$] followed by Tukey's post hoc test. (*E*) Quantification of pS129 α-synuclein protein levels in *C* normalized to α-synuclein monomer (17KD; $n = 3$). Significance was determined by two-way ANOVA [$F(3,24) = 11.08$; $P < 0.0001$] followed by a Tukey's post hoc test. Data are the mean ± SEM (*$P < 0.05$, **$P < 0.01$, and ***$P < 0.001$).

degree of overexpression achieved in DA neurons, or different genetic background. Many studies are terminated at 18 mo of age and are not carried out until 24 mo of age. By using a different approach, Liu et al. (11) generated Tet-sensitive LRRK2 GS transgenic mice under the direction of the PITX3 promoter to selectively drive LRRK2 expression in midbrain DA neurons. Although the authors achieved similar levels of LRRK2 GS expression as in our study, they only observed abnormalities in the DA system without degeneration of DA neurons. The reason for the difference is unclear but may be related to age, or perhaps expression in both DA and NE neurons is required for degeneration to occur (32). Interestingly, they find that PITX3 appears to be directly affected by LRRK2 transgene expression that likely lowers expression of LRRK2, which could have resulted in the lack of neurodegeneration in these mice. In the present study, transgene expression was activated after the animals were weaned to avoid potential developmental compensatory events that could prevent neurodegeneration.

A compelling observation is that LRRK2 GS induces a very robust reduction in the number of SVs and an accumulation of CCVs at synapses in vivo, suggesting a clathrin-dependent endocytic trafficking defect. Consistent with this notion are studies implicating LRRK2 in endocytic trafficking (reviewed in ref. 33). Other proteins with mutations linked to PD exhibit similar phenotypes, including Synaptojanin 1 (SJ1) (34) and α-synuclein (35), indicating that there are likely to be common molecular mechanisms that drive the synaptic phenotype. How LRRK2 GS promotes the accumulation of CCVs and the reduction of SVs needs to be explored in future studies. One possible link could be that LRRK2 regulates Endophilin and SJ1 by phosphorylation at synapses, which facilitates synaptic endocytosis through clathrin uncoating at the synaptic terminals (36–39). Future studies are required to determine whether these changes in synaptic integrity are causal or consequential.

The LRRK2 GS and LRRK2 GS/DA models described in the present study represent a substantial advance in animal genetic model development for LRRK2-associated PD. The development of LRRK2 GS/DA that expresses similar protein levels as the LRRK2 GS model confirms that kinase activity is critical for DA neurodegeneration. Moreover, the selective expression of LRRK2 GS in catecholaminergic neurons and the accompanying neurodegeneration indicates that LRRK2 GS kills catecholaminergic neurons in a cell-autonomous manner. It is likely that LRRK2 mutations in patients with PD kills catecholaminergic neurons in cell-autonomous and non–cell-autonomous fashions. This is supported by the findings that LRRK2 expression increases in activated microglia and reducing LRRK2 activity in microglia is neuroprotective (26–28). Additionally, these mice provide a robust and important platform to investigate molecular mechanisms for how DA neurons degenerate as a result of expression of LRRK2 GS. As the LRRK2 GS mice exhibit the accumulation of pathological, endogenous α-synuclein in an age-dependent manner, these animals are an important model to elucidate how LRRK2 GS contributes to α-synuclein pathology. Finally, these mice also are a platform to identify early molecular changes that could also provide new PD biomarkers, which would allow for the detection of the disease before symptom onset. In addition, they will support the evaluation of potential disease-modifying and neuroprotective therapies.

Materials and Methods

More detailed information on the study materials and methods is provided in *SI Materials and Methods*.

Animals. Mice were housed and treated in accordance with the National Institutes of Health (NIH) *Guide for the Care and Use of Laboratory Animals* (40) and institutional animal care and use committees of Johns Hopkins University and the National Cancer Institute.

Generation of TH-tTA Transgenic Mice. We constructed an hTH-tTA vector in which the human TH promoter (11 kb) drives expression of tTA and a fluorescent reporter zsGreen. Positive founders were selected and further subjected to semiquantitative PCR and normalized to GAPDH PCR to screen for high copy number founders. The three highest copy founders were selected and backcrossed with C57/BL6 mice for more than 10 generations and to establish the transgenic lines.

Immunohistochemistry. Mice were perfused with ice-cold PBS solution followed by ice-cold 4% paraformaldehyde (PFA; Sigma-Aldrich)/PBS solution (pH 7.4) and prepared for immunohistochemical staining as previously described (20).

Stereological Assessment of TH- and Nissl-Positive Cells. Unbiased stereological counting of TH-positive and Nissl-positive neurons was performed as previously described (21, 41).

Monoamine Analysis by HPLCy with Electrochemical Detection. Monoamine concentrations were measured by HPLC with electrochemical detection (HPLC-ECD) as previously described (21).

Western Blotting. Immunoblots were performed on brain tissue from the indicated genotype that homogenized in lysis buffer [1 × PBS, 1% Triton

X-100, 1× Complete protease inhibitor (4693116001; Sigma), 1× PhosSTOP phosphatase inhibitor (4906845001; Sigma)].

Transmission EM. Transmission EM (TEM) was performed on mouse brain slices at the microscope facility at The Johns Hopkins University School of Medicine.

Mouse Behavioral Tests. Spontaneous locomotor and exploratory activities were assessed by open-field test and d-amphetamine administration as described in our recent paper (20). The rotarod test to test motor coordination of mice was measured as the retention time on an accelerating rotarod of the Rotamex V instrument equipped with photo beams and a sensor to automatically detect mice that fell from the rotarod as described previously (20). The pole test, in which time to turn and time to descend is a sensitive measure of DA function, was performed as described previously (20). The gait analysis was performed by footprint analysis with stride length and stride width being measured.

Statistical Analysis. One-way or two-way ANOVA was used followed by a Tukey's or Dunnett's post hoc test as indicated for data analysis for multiple comparisons. *P* values for post hoc tests for each comparison are reported in Table S1. Data represent mean ± SEM, and $P \leq 0.05$ was considered statistically significant. Power analysis was performed by using G*Power 3.1 software to determine approximate sample sizes for stereological analysis or behavioral tests.

ACKNOWLEDGMENTS. This work was supported by NIH/National Institute on Aging (NIA) Grant K01-AG046366 (to Y.X.), William N. & Bernice E. Bumpus Foundation Innovation Awards (to Y.X.), American Parkinson Disease Association Research Grants (to Y.X. and X.M.), Kansas IDeA Network of Biomedical Research Excellence (Kansas INBRE) Grant P20 GM103418 (to Y.X.), Johnson Cancer Research Center Innovative Research Awards at Kansas State University (KSU; to Y.X.), startup funds and a Success for Young Investigators Intramural Grant from KSU College of Veterinary Medicine (to Y.X.), a National Science Foundation Graduate Research Fellowship Award (to J.C.G.), a Thomas Shortman Training Fund Graduate Scholarship Award (to J.C.G.), an Axol Science Scholarship Award (to J.C.G.), NIA Grants K01-AG056841 and ADRC P50AG005146 (to X.M.), NIH/National Institute of Neurological Disorders and Stroke Grants NS075839 (to L.I.), NS082205 (to H.S.K.), NS098006 (to H.S.K.), and NS38377 (to H.S.K., V.L.D., and T.M.D.), and the JPB Foundation (T.M.D.). The Confocal Core and Molecular Biological Core were supported by Kansas State University College of Veterinary Medicine. The authors acknowledge the joint participation by the Adrienne Helis Malvin Medical Research Foundation and the Diana Helis Henry Medical Research Foundation through direct engagement in the continuous active conduct of medical research in conjunction with The Johns Hopkins Hospital, the Johns Hopkins University School of Medicine, and the Foundation's Parkinson's disease Programs. T.M.D. is the Leonard and Madlyn Abramson Professor in Neurodegenerative Diseases.

1. Cookson MR (2010) The role of leucine-rich repeat kinase 2 (LRRK2) in Parkinson's disease. *Nat Rev Neurosci* 11:791–797.
2. Lees AJ, Hardy J, Revesz T (2009) Parkinson's disease. *Lancet* 373:2055–2066.
3. Martin I, Kim JW, Dawson VL, Dawson TM (2014) LRRK2 pathobiology in Parkinson's disease. *J Neurochem* 131:554–565.
4. Beccano-Kelly DA, et al. (2015) LRRK2 overexpression alters glutamatergic presynaptic plasticity, striatal dopamine tone, postsynaptic signal transduction, motor activity and memory. *Hum Mol Genet* 24:1336–1349.
5. Chen CY, et al. (2012) (G2019S) LRRK2 activates MKK4-JNK pathway and causes degeneration of SN dopaminergic neurons in a transgenic mouse model of PD. *Cell Death Differ* 19:1623–1633.
6. Garcia-Miralles M, et al. (2015) No dopamine cell loss or changes in cytoskeleton function in transgenic mice expressing physiological levels of wild type or G2019S mutant LRRK2 and in human fibroblasts. *PLoS One* 10:e0118947.
7. Herzig MC, et al. (2011) LRRK2 protein levels are determined by kinase function and are crucial for kidney and lung homeostasis in mice. *Hum Mol Genet* 20:4209–4223.
8. Li X, et al. (2010) Enhanced striatal dopamine transmission and motor performance with LRRK2 overexpression in mice is eliminated by familial Parkinson's disease mutation G2019S. *J Neurosci* 30:1788–1797.
9. Li Y, et al. (2009) Mutant LRRK2(R1441G) BAC transgenic mice recapitulate cardinal features of Parkinson's disease. *Nat Neurosci* 12:826–828.
10. Lin X, et al. (2009) Leucine-rich repeat kinase 2 regulates the progression of neuropathology induced by Parkinson's-disease-related mutant alpha-synuclein. *Neuron* 64:807–827.
11. Liu G, et al. (2015) Selective expression of Parkinson's disease-related Leucine-rich repeat kinase 2 G2019S missense mutation in midbrain dopaminergic neurons impairs dopamine release and dopaminergic gene expression. *Hum Mol Genet* 24:5299–5312.
12. Melrose HL, et al. (2010) Impaired dopaminergic neurotransmission and microtubule-associated protein tau alterations in human LRRK2 transgenic mice. *Neurobiol Dis* 40: 503–517.
13. Ramonet D, et al. (2011) Dopaminergic neuronal loss, reduced neurite complexity and autophagic abnormalities in transgenic mice expressing G2019S mutant LRRK2. *PLoS One* 6:e18568.
14. Tong Y, et al. (2009) R1441C mutation in LRRK2 impairs dopaminergic neurotransmission in mice. *Proc Natl Acad Sci USA* 106:14622–14627.
15. Tsika E, et al. (2014) Conditional expression of Parkinson's disease-related R1441C LRRK2 in midbrain dopaminergic neurons of mice causes nuclear abnormalities without neurodegeneration. *Neurobiol Dis* 71:345–358.
16. Volta M, et al. (2015) Chronic and acute LRRK2 silencing has no long-term behavioral effects, whereas wild-type and mutant LRRK2 overexpression induce motor and cognitive deficits and altered regulation of dopamine release. *Parkinsonism Relat Disord* 21:1156–1163.
17. Weng YH, et al. (2016) (R1441C) LRRK2 induces the degeneration of SN dopaminergic neurons and alters the expression of genes regulating neuronal survival in a transgenic mouse model. *Exp Neurol* 275:104–115.
18. Yue M, et al. (2015) Progressive dopaminergic alterations and mitochondrial abnormalities in LRRK2 G2019S knock-in mice. *Neurobiol Dis* 78:172–195.
19. Xiong Y, Dawson TM, Dawson VL (2017) Models of LRRK2-associated Parkinson's disease. *Adv Neurobiol* 14:163–191.
20. Xiong Y, et al. (2017) Overexpression of Parkinson's disease-associated mutation LRRK2 G2019S in mouse forebrain induces behavioral deficits and α-Synuclein pathology. *eNeuro* 4:ENEURO.0004-17.2017.
21. Karuppagounder SS, et al. (2016) LRRK2 G2019S transgenic mice display increased susceptibility to 1-methyl-4-phenyl-1,2,3,6-tetrahydropyridine (MPTP)-mediated neurotoxicity. *J Chem Neuroanat* 76:90–97.
22. Galter D, et al. (2006) LRRK2 expression linked to dopamine-innervated areas. *Ann Neurol* 59:714–719.
23. Higashi S, et al. (2007) Localization of Parkinson's disease-associated LRRK2 in normal and pathological human brain. *Brain Res* 1155:208–219.
24. Melrose H, Lincoln S, Tyndall G, Dickson D, Farrer M (2006) Anatomical localization of leucine-rich repeat kinase 2 in mouse brain. *Neuroscience* 139:791–794.
25. West AB, et al. (2014) Differential LRRK2 expression in the cortex, striatum, and substantia nigra in transgenic and nontransgenic rodents. *J Comp Neurol* 522: 2465–2480.
26. Daher JP, Volpicelli-Daley LA, Blackburn JP, Moehle MS, West AB (2014) Abrogation of α-synuclein-mediated dopaminergic neurodegeneration in LRRK2-deficient rats. *Proc Natl Acad Sci USA* 111:9289–9294.
27. Moehle MS, et al. (2012) LRRK2 inhibition attenuates microglial inflammatory responses. *J Neurosci* 32:1602–1611.
28. Thévenet J, Pescini Gobert R, Hooft van Huijsduijnen R, Wiessner C, Sagot YJ (2011) Regulation of LRRK2 expression points to a functional role in human monocyte maturation. *PLoS One* 6:e21519.
29. Kessler MA, Yang M, Gollomp KL, Jin H, Iacovitti L (2003) The human tyrosine hydroxylase gene promoter. *Brain Res Mol Brain Res* 112:8–23.
30. Tumbar T, et al. (2004) Defining the epithelial stem cell niche in skin. *Science* 303: 359–363.
31. Chen ZC, et al. (2017) Phosphorylation of amyloid precursor protein by mutant LRRK2 promotes AICD activity and neurotoxicity in Parkinson's disease. *Sci Signal* 10: eaam6790.
32. Rommelfanger KS, et al. (2007) Norepinephrine loss produces more profound motor deficits than MPTP treatment in mice. *Proc Natl Acad Sci USA* 104: 13804–13809.
33. Abeliovich A, Gitler AD (2016) Defects in trafficking bridge Parkinson's disease pathology and genetics. *Nature* 539:207–216.
34. Cao M, et al. (2017) Parkinson Sac domain mutation in synaptojanin 1 impairs clathrin uncoating at synapses and triggers dystrophic changes in dopaminergic axons. *Neuron* 93:882–896.e885.
35. Nemani VM, et al. (2010) Increased expression of alpha-synuclein reduces neurotransmitter release by inhibiting synaptic vesicle reclustering after endocytosis. *Neuron* 65:66–79.
36. Islam MS, et al. (2016) Human R1441C LRRK2 regulates the synaptic vesicle proteome and phosphoproteome in a Drosophila model of Parkinson's disease. *Hum Mol Genet* 25:5365–5382.
37. Soukup SF, et al. (2016) A LRRK2-dependent Endophilin A phosphoswitch is critical for macroautophagy at presynaptic terminals. *Neuron* 92:829–844.
38. Arranz AM, et al. (2015) LRRK2 functions in synaptic vesicle endocytosis through a kinase-dependent mechanism. *J Cell Sci* 128:541–552.
39. Matta S, et al. (2012) LRRK2 controls an EndoA phosphorylation cycle in synaptic endocytosis. *Neuron* 75:1008–1021.
40. National Research Council (2011) *Guide for the Care and Use of Laboratory Animals* (National Academies Press, Washington, DC), 8th Ed.
41. Lee Y, et al. (2013) Parthanatos mediates AIMP2-activated age-dependent dopaminergic neuronal loss. *Nat Neurosci* 16:1392–1400.